



Research article

NANO-SBT-PEDF delivery system: A promising approach against ovarian cancer?

Pascale Ribaux^{a,b}, Christine Wuillemin^{a,b}, Patrick Petignat^b, Florence Delie^{c,d}, Marie Cohen^{a,b,*}^a Translational Research Centre in Onco-Hematology, University of Geneva, Geneva, Switzerland^b Department of Pediatric, Gynecology and Obstetrics, University of Geneva, Geneva, Switzerland^c Institute of Pharmaceutical Sciences of Western Switzerland, University of Geneva, Rue Michel-Servet 1, 1211, Geneva, Switzerland^d School of Pharmaceutical Sciences, University of Geneva, Rue Michel-Servet 1, 1211, Geneva, Switzerland

ARTICLE INFO

Keywords:

Sleeping beauty transposon
PEDF
Liposome
Lipid nanoparticle
Ex vivo ovarian tumor model

ABSTRACT

Pigment epithelium-derived factor (PEDF) is a secreted glycoprotein involved in various biological processes. Its expression declines during ovarian carcinogenesis where it could decrease macrophages polarization, inhibit angiogenesis and induce apoptosis. Altogether, PEDF represents an ideal anti-cancer agent against ovarian cancer. We previously proposed the non-viral Sleeping Beauty transposon (SBT) system to stably integrate the PEDF transgene into ovarian cancer cells. Here, we report the development of liposomes and lipid nanoparticles for SBT-PEDF gene therapy. We determined that the SBT-PEDF nanolipid delivery system was the best system to increase the expression of PEDF in ovarian cancer spheroids. We also developed an ex vivo model of ovarian tumors which allowed us to show that nanolipoplexe in combination to paclitaxel exhibits synergistic and effective anti-tumor efficacy on ovarian tumors. These findings demonstrate that lipid nanoparticle for SBT-PEDF gene therapy may be a promising therapeutic approach for ovarian cancer.

1. Introduction

Ovarian cancer is the fifth leading cause of cancer-related death in the world and has the highest mortality of any of the gynecologic cancers. The most common form of ovarian cancer is the epithelial ovarian carcinoma. Current treatments of advanced ovarian carcinoma are surgical resection and combinatory chemotherapy. Initially, more than 70% of treated patients respond positively to treatment; however, in about 70% of patients the cancer reoccurs and is resistant to treatment. Late-stage disease and relative resistance to chemotherapy displayed by most ovarian cancer represent a significant clinical challenge.

Pigment epithelium-derived factor (PEDF; encoded by SERPINF1) is a 50-kDa secreted glycoprotein belonging to the supergene family of serpins (serine protease inhibitors). PEDF has several biological activities, which depend on its interactions with cell surface receptors (PEDF receptor encoded by PNPLA2, laminin receptor, F₁ ATPase/synthase and low-density lipoprotein receptor-related protein 6) and their downstream signaling pathways [1,2].

PEDF is involved in various biological processes, such as organogenesis and tissue homeostasis maintenance. PEDF is also a potent inhibitor of angiogenesis by increasing gamma-secretase activity, an enzyme that cleaves the vascular endothelial-derived growth

* Corresponding author. Translational Research Centre in Onco-Hematology, University of Geneva, Geneva, Switzerland.
E-mail address: marie.cohen@unige.ch (M. Cohen).

factor (VEGF) receptor (VEGFR, [1,3]). PEDF can also upregulate presenilin 1 expression, which facilitates the association between tyrosine phosphatases and VEGFR to inhibit VEGF-induced phosphorylation of VEGFR [1,3]. In addition, PEDF suppresses endothelial cell migration via p38 MAPK pathway activation and induces endothelial cell apoptosis by activating peroxisome proliferator-activated receptor gamma to induce TP53 expression, and Fas-FasL-caspase 8 pathway [1,3].

PEDF level declines during ageing [4] and carcinogenesis in various types of cancers including ovarian cancer [5–7]. Exogenous PEDF inhibits the growth of ovarian surface epithelium and ovarian cancer cell lines [5]. It also induces response to paclitaxel treatment, and decreases ovarian tumor development on chick allantoid membrane assay by inducing apoptosis and inhibiting angiogenesis [7]. These observations suggest that the decrease of PEDF expression could contribute to early ovarian carcinogenesis. To reinforce this hypothesis, PEDF expression is significantly negatively correlated with progression of ovarian cancer [8].

More recently, a role of PEDF on macrophages polarization in different types of cancer [9,10], including ovarian cancer [8], is emerging. It was shown that the overexpression of PEDF leads to the inhibition of ovarian cancer tumor growth and tumor-associated macrophages polarization through adipose triglyceride lipase (ATGL) and ERK1/2 [8]. In addition, PEDF level is significantly and negatively correlated with tumor-associated macrophage polarization. M1 and M2 macrophage polarization is a physiological process associated with different macrophage functions. Macrophages infiltrating tumors have been described as M2 phenotype. This phenotype is associated with tumor progression and immunosuppression, by promoting tumor angiogenesis, tumor metastasis, and suppression of tumor immunity [11]. Altogether, these observations suggest that PEDF may also be useful in ovarian cancer immunotherapy.

Due to its various roles, PEDF has been proposed as an anti-cancer agent against a range of tumors including ovarian tumors [1,3]. Three different strategies were used to increase PEDF level in tumors environment.

- 1 the systemic administration of PEDF protein or active PEDF peptides [12–18],
- 2 the PEDF gene therapy by delivering the PEDF gene using different techniques (Table 1) and
- 3 the cell-based therapy using PEDF virally infected human mesenchymal cells [19–21].

A number of efficient methods to deliver PEDF gene have been developed including viral vectors, microparticles and nanoparticles (NP) of various compositions [1]. To increase anti-tumor efficiency, some targeted PEDF gene delivery systems have also been developed (Table 1). However, efforts are still needed to avoid both continuous administration of PEDF peptides/protein or gene to sustain its expression in tumor environment.

We previously used the non-viral Sleeping Beauty transposon (SBT) system to stably integrate the PEDF transgene into SKOV3 ovarian cancer cells [7]. The transfected cells maintained PEDF expression for at least 6 months, suggesting that this SBT-PEDF system could be used to maintain PEDF level in tumor environment [7]. Here, we report the development of different delivery systems such as cationic liposomes and cationic lipid nanoparticles for SBT-PEDF gene therapy to select the best one. The efficacy of selected candidate was tested in a novel ex vivo ovarian tumor assay.

2. Material and methods

2.1. Material

The miniaturized spinning bioreactors, SpinΩ, were purchased from 3Dynamics (Baltimore, MD, USA).

Table 1
PEDF gene therapy delivery systems as a therapeutic tool against cancer.

Vehicle	Target	Ligand	Content	Cancer	Animal model	Ref.
PLGA NP			PEDF gene	Colon carcinoma	CT26 tumor bearing mice	[22]
PEG-PEI NP	Integrin $\alpha\beta 3$ receptor	Cyclic RGD peptide	PEDF gene	Colon carcinoma	SW620 tumor bearing mice	[23]
Adeno-associated virus			PEDF gene	Lewis lung carcinoma	LLC tumor bearing mice	[24]
Cationic liposome			Recombinant PEDF adenovirus	Melanoma	B16–F10 tumor bearing mice	[25]
PEG-PLGA NP			PEDF gene	Colon carcinoma	CT26 tumor bearing mice	[26]
PEG-PLGA NP	FGFR1	Truncated bFGF peptide	Ptx + PEDF gene	Colon carcinoma	CT26 tumor bearing mice	[27]
MAL-PEG-DSPE	Integrin $\alpha\beta 3$	Cys-iRGD	PEDF gene	Colon carcinoma	CT26 tumor bearing mice	[28]
PEG-Chol nanoliposome	Folate receptor	Folic acid	PEDF gene	Cervical cancer	Hela tumor bearing mice	[29]

Chol: cholesterol, DSPE: 1,2-Distearoyl-sn-glycero-3-phosphorylethanolamine, MAL: maleimide, NP: nanoparticle, PEG: polyethylene glycol, PEI: polyethylene imine, PLGA: poly-lactide-co-glycolic acid, Ptx: paclitaxel.

2.2. Plasmids

Plasmids used to construct the SBT-PEDF system were.

- pCMV3-SERPINF1 (# HG11104-UT) from Sino Biological Inc.
- pSBbi-GN (# 60517) from Addgene (contains a GFP tag)
- pCMV(CAT)T7-SB100 (# 34879) from Addgene

The plasmid pSBbi-GN was the control (CTRL) transposon and pCMV(CAT)T7-SB100 was the transposase.

The plasmid pSBbi-GN-PEDF, used as PEDF transposon, was generated by cloning the insert of the human PEDF sequence from pCMV3-SERPINF1 into HindIII-XbaI restriction site of pSBbi-GN.

2.3. Chemical products

18:1 (Δ^9 -Cis) PE (DOPE) 1,2-dioleoyl-sn-glycero-3-phosphoethanolamine was from Avanti Polar Lipids Inc.

18:1 TAP (DOTAP) 1,2-dioleoyl-3-trimethylammonium-propane (chloride salt) was from Avanti Polar Lipids Inc.

Poly(D,L-lactic-co-glycolic acid) (PLGA, resomer RG502H) was from Evonik, Germany.

Polyvinyl alcohol (PVAL) 31 kDa MOWIOL 4-88 was obtained from Clariant, Germany.

Protamine sulfate, cholesterol and MTT reagent were from Sigma-Aldrich.

The control transfection reagent JetPei was from Polyplus transfection (Illkirch, France).

The ELISA kit for human PEDF detection was from BioProductsMD (Frederick, MD, USA).

The HistoGel for spheroids embedding was from Histocom AG (Zug, Switzerland).

Anti-active caspase-3 antibodies (#9661) and anti-GFP antibodies (ab13970) were respectively from Cell Signaling Technology (Leiden, The Netherlands) and Abcam (Cambridge, United Kingdom).

2.4. Cell lines

Experiments were performed on the human ovarian carcinoma cell lines SKOV3 (American Type Culture Collection ATCC, Manassas, VA) and COV318 (ECACC, Sigma-Aldrich). SKOV3 and COV318 cells were cultured in respectively RPMI or DMEM medium (Gibco, Invitrogen, Basel, Switzerland) supplemented with 10% fetal bovine serum (FBS) and gentamicin (Gibco, Invitrogen, Basel, Switzerland).

2.5. Liposome preparation

Liposomes were generated with a combination of lipids following a protocol adapted from the lipid supplier (Avanti Polar Lipids Inc.).

Briefly, lipids were dissolved in chloroform and mixed in a glass vial that rotated in a water-bath at 45 °C (Rotavapor, Buchi, Switzerland). The chloroform was evaporated with a vacuum pump and the lipid film was resuspended in water prewarmed at 54 °C. Saline buffer (308 mM NaCl, 40 mM Hepes, pH 7.4) was added to the suspension (final concentration of 5 mg/ml of lipids) that was sonicated for 5 min at 50% intensity (sonifier S-450D®, Branson Ultrasonic S.A, Switzerland) and passed through a 0.22 μ m filter to sterilize.

2.6. Cationic lipid nanoparticle preparation

Cationic lipid nanoparticles (nanolipids) were generated with the double-emulsion method described by Bose et al. [30].

Briefly, the organic phase contained PLGA (3% w/v) and DOTAP (24% w/w to polymer) dissolved in dichloromethane. The water-in-oil emulsion was formed by the addition of deionized water containing or not protamine sulfate (10 μ g/ml) into the organic phase with sonication in an ice bath for 5 min at 50% intensity. The primary emulsion was then transferred to 1% w/v PVAL aqueous solution and sonicated again in an ice bath. The resultant secondary (water in oil in water) emulsion was stirred overnight at room temperature. After complete evaporation of dichloromethane, the nanolipids were centrifuged at 20 000 rpm for 30 min (Avanti®30 Centrifuge, Beckman Coulter Inc., Fullerton, CA, USA), washed three times in deionized water, resuspended in deionized water at a concentration of 10 mg/ml, and kept at 4 °C until use.

2.7. Characterization of delivery systems

The mean particle diameter (z-average), size distribution (polydispersity index) and the ζ -potential of delivery systems were determined using a Zetasizer Nano ZS (Malvern Instruments, Malvern, United Kingdom).

2.8. Formation of DNA-delivery system and gel retardation assay

Plasmid DNA incorporation efficiency was verified by gel retardation assay. A mixture of 1 μ g total DNA of transposase/transposon

PEDF (ratio 1:19) was incubated with liposome or nanolipids in phosphate-buffered saline (PBS). Different combinations of DNA/liposome or nanolipids ratio were tested to form lipoplexes or nanolipoplexes, respectively. After incubation for 30 min at room temperature, the mixture was centrifuged 4 min at 10 000 rpm and loading buffer (0.25% w/w bromophenol blue in TE buffer) was added to the complexes, which were applied to 1% agarose gel prepared using Basic agarose premier (MP Biomedicals, Illkirch, France). Electrophoresis was carried out at 100 V for 20 min at room temperature in $0.5 \times$ TAE buffer. The gels were stained with SYBR Safe DNA gel stain, as indicated by the manufacturer (Cartshad, CA, USA). Acquisition was accomplished using the GeneFlash machine (Syngene Bioimaging).

2.9. MTT assay

Cells were seeded in 96-well plates at a density of 15 000 cells/well. After 24 h, transfection was performed using either empty liposomes, lipoplexes, nanolipids or nanolipoplexes with 150 ng total pDNA.

The CTRL transposon plasmid was used instead of the PEDF transposon plasmid to avoid the potential bias effect of the PEDF gene on cell viability. The cell survival was assessed 48 h post-transfection by MTT assay, following manufacturer's instructions. Briefly, 48 h post transfection, the medium was replaced with a medium containing 20% MTT solution (5 mg/mL in medium) for 2 h. Acidic isopropanol solution (150 μ L) was added, and then each well was vigorously mixed to dissolve the precipitated formazan. UV-visible absorption was measured at 540 and 690 nm. Cell viability assay was performed for three independent experiments, run in triplicate.

2.10. Transfection of 2D and 3D ovarian cancer cells

2.10.1. Transfection of 2D ovarian cancer cells

300'000 cells were seeded in 6-well plates in complete medium. The next day, pDNA/liposome (at ratio 1:1, 1:3, 1:6, 1:8 and 1:10) or cationic lipid nanoparticle (at ratio 1:60) were incubated at room temperature for 30 min. Meanwhile, the cells were washed 2 times with HBSS and lipoplexes or nanolipoplexes were added dropwise to cells maintained in serum-free medium. Different incubation times of nanolipoplexes (4 h, 6 h or overnight at 37 °C) were tested. After the incubation time, cells were washed, and complete medium was added. The cells were harvested 48 h post-transfection.

To evaluate the relative transfection efficiency of our delivery systems, we also transfected cells with JetPei (as positive control of transfection). JetPei-pDNA complexes were prepared according to manufacturer's instructions and equalized to our experimental conditions.

2.10.2. Transfection of 3D ovarian cancer cells

96-round bottom well plates were coated with 60 μ L/well of poly-HEMA solution at 12 mg/ml in 95% ethanol. The coating was performed twice to ensure homogenous poly-HEMA layer. Plates were kept at 4 °C until use and sterilized for 10 min under UV light before SKOV3 and COV318 cells were seeded with multichannel pipet at a density of 20 000 cells/well in culture medium supplemented with 5% FBS.

Two days after cell seeding, the same number of spheroids (7–15 per experiment) were transferred into 12-well poly-HEMA plates. Four different transfection conditions for each cell line were tested.

- control (no transfection),
- JetPei (positive control transfection reagent used at 2 μ L/ μ g of DNA)
- liposome 1
- nanolipid 1

Transfection was performed using 1 μ g total DNA/100 000 cells (i.e. 3 μ g for 15 spheroids). A single combination of DNA/vector ratio was tested: 1:6 for liposome 1 and 1:60 for nanolipid 1.

A double transfection was performed for each condition at day 2 and day 4 in 12-well plates with the following protocol. Culture medium was aspirated, and 0.5 ml of fresh medium was added. The different transfection mixtures were incubated for 30 min and added dropwise to appropriate wells. Then fresh medium (0.5 ml) was added to each well 6 h post-transfection.

At day 7, spheroids were harvested for RNA extraction.

2.11. Transfection on ovarian tumors

2.11.1. Development of an ex vivo tumor assay

The first step was to develop SKOV3 tumors on chicken chorioallantoic membrane as previously described [7]. It is important to note that the incubation of eggs did not exceed 14 days (or embryonic development day 14) to avoid ethical restrictions. These experiments were conducted in accordance with institution guidelines and EU directive 2010/63/EU for animal experiments. Briefly, SKOV3 cells were inoculated on chicken chorioallantoic membrane (CAM, 2×10^6 cells per egg) and left for 6 days to form tumors. Tumors were then collected from CAM and cultured in 12-well plates covered by a miniaturized spinning bioreactor (spin Ω). Medium supplemented with 10% or 20% FBS was changed every 2 days and after 8 days in culture, tumors were washed in PBS, fixed in formol and paraffin-embedded for histological analysis.

2.11.2. Transfection of *ex vivo* ovarian tumors

SKOV3-derived tumors were cultured for 7 days and transfected 4 times with the CTRL transposon or the PEDF transposon (6 μ g total DNA) using the cationic lipid nanoparticle “nanolipid 1” at a ratio DNA:nanolipid 1:60 (w:w) at day 0, 1, 4 and 5. Tumors were treated or not with paclitaxel (10 μ M) for 24 h at day 6. Tumors will be then washed in PBS, fixed in formol and, paraffin embedded for histological analysis.

2.12. RT-qPCR

Total RNA extraction was achieved with the PureLink RNA mini kit (Invitrogen). Reverse transcription was performed with 1 μ g of total RNA using the High-Capacity cDNA Reverse Transcription Kit (Applied Biosystems, Life Technologies). Detection of the real-time qPCR product was performed using the KAPA SYBR FAST qPCR Kit Master Mix (Kapa Biosystems, Axon Lab, Baden, Switzerland) on an Eco Real-Time PCR System (Labgene Scientific, Châtel-St-Denis, Switzerland). Level of PEDF mRNA expression was measured by qPCR and normalized with 3 different housekeeping genes (GAPDH, HPRT1 and cyclophilin A, Table 2). Normalization of RT-qPCR data using three reference genes was performed with the geometric mean of the multiple reference genes. Results were expressed as means \pm SEM (n = 3 experiments).

2.13. Immunofluorescence

Slices of 5 μ m of ovarian tumors were cut and labeled with anti-GFP antibodies (1/500; overnight, 4 °C). They were then washed with PBS three times and incubated with secondary antibodies anti-chicken-488 (dilution 1:500) diluted in PBS-3% BSA for 2 h at room temperature. Slices were washed four times in PBS and mounted with Vectashield with DAPI (Vector Laboratories, Burlingame, USA). Images were acquired with an EVOS FL Cell Imaging System (ThermoFisher scientific, Bothell, WA, USA).

2.14. Histology

Slices of 5 μ m were cut and stained for hematoxylin and eosin (H&E) and active caspase-3 as proposed by Bonnet to evaluate the structural aspect and the viability of the tumors [31]. We evaluated the percentage of cells positive for caspase 3 staining on each slide and categorized them as negative, positive with less than 5% of caspase 3-positive cells or positive with more than 5% of caspase 3-positive cells.

2.15. Statistical analysis

Data are represented as means \pm standard error of the mean (SEM) for three different replicates. Statistical differences between samples or tested conditions were assessed by the unpaired Student's *t*-test or analysis of variance (ANOVA). A significance level of $p < 0.05$ was considered statistically significant. Statistical analyses were performed using GraphPad Prism 8 (GraphPad Software, San Diego, USA).

3. Results

Cationic liposomes are usually composed of a cationic lipid and neutral helper lipids such as cholesterol and DOPE [32]. We thus tested these two molecules in combination with DOTAP to produce cationic liposomes.

DOTAP was also used in combination with PLGA to produce lipid nanoparticle. The different liposomes and cationic lipid nanoparticles (nanolipids) were produced by respectively the film dispersion method and the double emulsion solvent evaporation method as described previously.

3.1. Characterization of liposomes and cationic lipid nanoparticles

The mean particle diameter (average size), size distribution (average polydispersity) and zeta potential of liposome 1 and 2 are quite similar (Table 3). Liposome 3 average size is a little bit larger than liposomes 1 and 2. Nanolipids present an average size and size distribution in the similar range as liposomes. Their zeta potential is lower compared with liposomes suggesting that their capacity to bind plasmid with negatives charges could be decreased compared with liposomes.

Table 2
qPCR primers sequences.

Gene name	Forward sequence	Reverse sequence
PEDF	5'-TTA CGA AGG CGA AGT CAC CA-3'	5'-TAA GGT GAT AGT CCA GCG GG-3'
HPRT1	5'-ATG ACC AGT CAA CAG GGG AC-3'	5'-TGC CTG ACC AAG GAA AGC AA-3'
GAPDH	5'-CGA CCA CTT TGT CAA GCT CA-3'	5'-CCC TGT TGC TGT AGC CAA AT-3'
Cyclophilin A	5'-TAC GGG TCC TGG CAT CTT GT-3'	5'-CCA TTT GTG TTG GGT CCA GC-3'

3.2. pDNA loading capacity of liposomes and lipid nanoparticles

The encapsulation efficiency of the plasmid was then determined by agarose gel electrophoresis (Fig. 1). The naked PEDF-DNA exhibited a bright band on the gel. The plasmid is considered completely packaged by the liposome or nanolipid when the DNA band is not visible on the gel. In this case, the plasmids-loaded liposome (lipoplexes) or nanolipid (nanolipoplexes) remain in the loading hole. We thus determined the ratio pDNA:delivery system for each liposome and nanolipid formulation allowing complete encapsulation of pDNA: 1:6 for liposomes, and 1:60 for nanolipid 1. The addition of protamine in nanolipid 2 preparation seems to have decreased the encapsulation capacity of the nanolipid since DNA remains visible even at a ratio pDNA:nanolipid 1:150.

3.3. Cytotoxicity of liposomes and lipoplexes

Cytotoxicity is an important problem associated with lipoplexes, limiting their clinical use. The cytotoxicity of liposomes 1 to 3 and their corresponding lipoplexes at different DNA:liposomes ratio was investigated with SKOV3 and COV318 cells by MTT assays. As shown in Fig. 2, the cytotoxicity of lipoplexes 2 and 3 was confirmed in all conditions. The cytotoxicity of lipoplexe 1 depends on pDNA:liposome 1 ratio. The ratio pDNA:liposome 1, which allows the complete incorporation of DNA in liposome, altered cell viability of COV318 cells but not SKOV3 cells.

3.4. Efficiency of liposomes

We then investigated the expression of PEDF mRNA by RT-qPCR to check the effects of liposome/SBT-PEDF gene delivery systems at ratio 1:6, 1:8 and 1:10 (Fig. 3). The results showed that the increase in PEDF gene expression with these delivery systems is negligible compared with the commercial transfection reagent JetPei in both SKOV3 and COV318 cells (Fig. 3, left panels). Nevertheless, they could increase PEDF mRNA expression in these ovarian cancer cells (Fig. 3, right panels). In addition, we cannot observe any difference in PEDF expression regardless of the tested pDNA:liposome ratio.

3.5. Cytotoxicity and efficiency of nanolipids

Cationic lipid PLGA nanoparticles were also described as more cytotoxic than PLGA nanoparticles due to their positive charges. We thus evaluated cytotoxicity of nanolipids 1 and 2 and the corresponding nanolipoplexes in ovarian cancer cells using the highest pDNA:nanolipid ratio which allowed the complete encapsulation of DNA (1:60, w:w). Cells were incubated with pDNA:nanolipid complexes for 4 h, 6 h and overnight before culture medium change to determine the best conditions of transfection. As shown in Fig. 4A, the addition of protamine in nanolipid 2 seems to significantly decrease the cytotoxicity of nanolipids in both SKOV3 and COV318 cells. However, it does not reduce the cytotoxicity of nanolipoplexes.

The expression of PEDF mRNA showed that the increase in PEDF gene expression with these delivery systems is negligible compared with the commercial transfection reagent JetPei in both SKOV3 and COV318 cells (Fig. 4B, left panels). Nevertheless, they could increase PEDF mRNA expression in these ovarian cancer cells regardless of the tested incubation time (Fig. 4B, right panels). Surprisingly, the increase in PEDF expression in both cell lines is more important with nanolipoplexe 1 than with nanolipoplexe 2, which contains protamine sulfate (often used in gene delivery system for the stabilization and delivery of nucleic acids [33]).

3.6. Efficiency of liposome 1 and nanolipid 1 on ovarian cancer spheroids

The efficiency of the best lipoplexe and nanolipoplexe formulations was then evaluated on ovarian cancer spheroids. Considering previous results, we chose lipoplexe 1 at a ratio 1:6 (pDNA:liposome, w:w), nanolipoplexe 1 at a ratio 1:60 and JetPei reagent to transfect SKOV3 and COV318 spheroids with SBT-PEDF system. The expression of PEDF mRNA by RT-qPCR showed that nanolipid 1 is the most efficient to increase PEDF expression in ovarian cancer spheroids (Fig. 5A). Unexpectedly, the transfection of spheroids with nanolipoplexe 1 was also more efficient to increase PEDF expression in ovarian cancer spheroids than in 2D cultured cells.

We next evaluated the cytotoxicity of nanolipoplexe 1 on SKOV3 and COV318 spheroids. As observed in Fig. 5B, transfection of SBT-CTRL or SBT-PEDF system with nanolipid 1 did not alter cell viability of both SKOV3 and COV318 spheroids.

Table 3

Characterization of liposomes and cationic lipid nanoparticles.

Delivery system	Composition	Average size (nm)	PDI	Average Zeta potential (mV)	SD Zeta potential
Liposome 1	DOPE/DOTAP (1/3 M ratio)	184	0.163	76	9
Liposome 2	DOTAP/cholesterol (3/1 M ratio)	181	0.167	78	13
Liposome 3	DOPE/DOTAP/cholesterol (1/4/1 M ratio)	233	0.209	78	10
Nanolipid 1	PLGA/DOTAP (24% w:w)	162	0.127	52	7
Nanolipid 2	PLGA/DOTAP (24% w:w)/protamine	203	0.184	50	6

PDI: polydispersity index, w: weight.

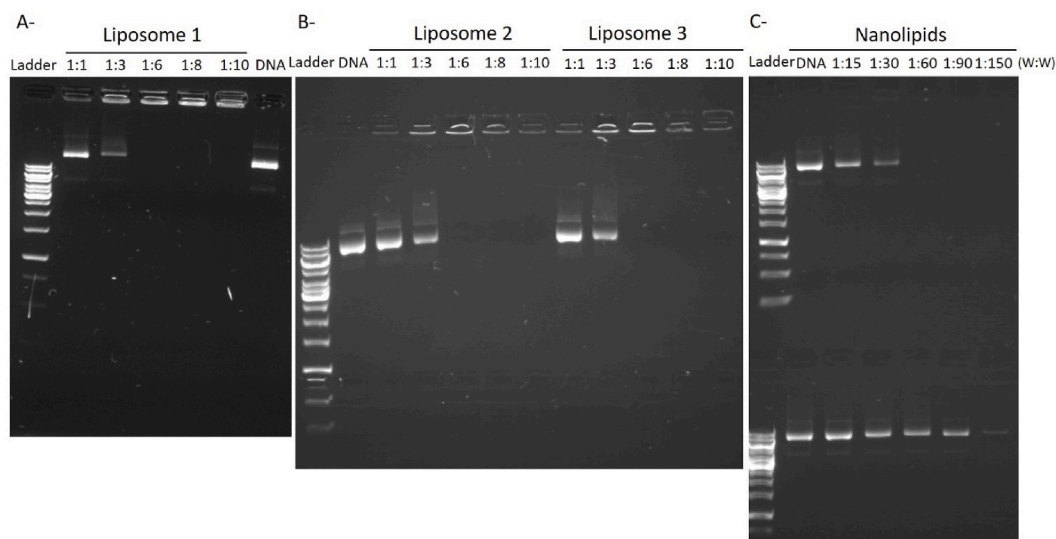


Fig. 1. pDNA loading capacity of liposomes and lipid nanoparticles. Different pDNA:delivery system ratio (weight:weight; w:w) were used to determine the pDNA loading capacity of liposome 1 (A), 2 and 3 (B), and nanolipid 1 (C, upper gel) and 2 (C, lower gel). pDNA alone was used as positive control on the agarose gels.

3.7. Development of an *ex vivo* tumor assay

Finally, we developed an *ex vivo* tumor assay to evaluate the efficacy of nanolipid 1 to deliver gene.

The first step was to develop SKOV3 tumors on chicken chorioallantoic membrane (CAM, Fig. 6A). Tumors were then extracted and cultured in 12-well plates covered by a miniaturized spinning bioreactor (spinΩ). The use of this bioreactor should allow to maintain the tumor structure and viability, and consider the effects of shear stress on transfection efficiency in case this therapy would be applied intraperitoneally. Indeed, the presence of malignant ascites in peritoneal cavity is often observed in ovarian cancer patients and is associated to hydrostatic compression and shear stress [34]. Culture medium supplemented with 10% or 20% FBS was changed every 2 days. After 8 days in culture, tumors were fixed in formol, and paraffin embedded for H&E and active caspase-3 staining to evaluate the structural aspect and the viability of the tumors. Representative tumors are shown in Fig. 6B–D. The staining of tumors cultured in bioreactor was less eosinophil than that of tumors just extracted from the CAM, but the structural aspect of the tumors remained similar. Some clusters of apoptotic cells were sometimes present in the core of the tumors independently of the percentage of FBS used in the culture medium, but the tumors were still viable after 8 days of culture.

3.8. Efficiency of nanolipoplexes 1 on plasmids transfection in ovarian tumors

Based on these observations, we used this *ex vivo* tumor assay to perform transfection experiments on SKOV3-derived tumors.

After dissection, tumors were cultured for 7 days and transfected 4 times with the CTRL transposon or the PEDF transposon using the nanolipid 1 at day 0, 1, 4 and 5. Tissues were then labeled with anti-GFP antibodies to evaluate the transfection efficiency. As positive control, we used a tumor extracted from CAM, which was obtained after inoculation of SKOV3 cells stably transfected with CTRL transposon (as described in Ref. [7]). As observed in Fig. 7, tumor extracted from CAM is positive for GFP staining in contrast to the surrounding tissue, which is the allantoic membrane. Tumor transfected with nanolipoplexe 1 is also positive for GFP staining confirming the efficiency of transfection.

3.9. Effect of PEDF on paclitaxel-treated ovarian tumors

We then treated transfected tumors with paclitaxel to evaluate the effect of PEDF overexpression on paclitaxel-induced apoptosis of tumors. As shown in Fig. 8, tumors transfected with PEDF transposon (Fig. 8A and C) were more often and more positively stained for cleaved caspase 3 than tumors transfected with ctrl transposon (Fig. 8B and C), which are mostly negative for cleaved caspase 3.

4. Discussion

PEDF is known as a promising candidate for inhibiting ovarian tumor growth due to its ability to exert anti-angiogenic and pro-apoptosis effects. More recently, it was shown that PEDF could also inhibit tumor-associated macrophages polarization suggesting that PEDF could also modulate tumor immunity. Altogether, PEDF represents an ideal therapeutic candidate against ovarian tumors. Two main strategies have already been described to evaluate PEDF as a therapeutic agent: the PEDF gene therapy using viral vectors

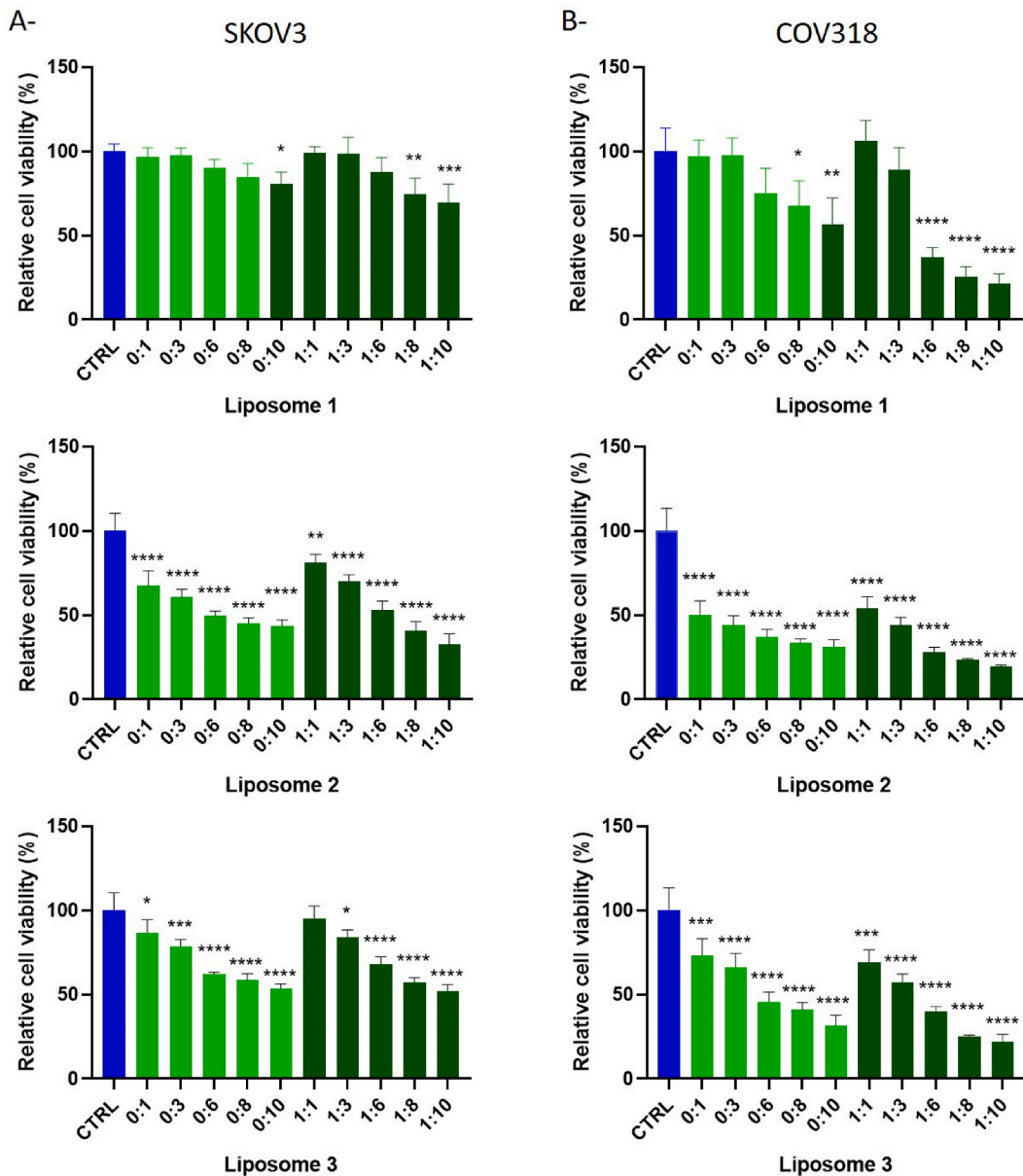


Fig. 2. Cytotoxicity of liposomes and lipoplexes. Effect of liposomes (light green) and lipoplexes (dark green) on viability of SKOV3 (A) and COV318 cells (B) was evaluated by MTT assay. Results are expressed as mean ± SEM, n = 3. *p < 0.05; **p < 0.01; ***p < 0.001; ****p < 0.0001 compared to the control (CTRL, in blue).

and systemic administration of PEDF proteins or peptides. Despite these approaches confirm the efficiency of PEDF against different types of cancer, they are not useable for clinical application. We thus decided to develop a cost-effective therapeutic strategy to induce and sustain PEDF expression in tumor environment, using the Sleeping Beauty Transposon system to stably introduce PEDF in the genome of ovarian cancer cells. In this study, we developed different SBT-PEDF gene delivery systems for the treatment of ovarian cancer and investigated their efficiency to increase PEDF expression in vitro both in 2D and 3D cultured cells and an ex vivo model to evaluate the efficiency of the best SBT-PEDF gene delivery system to enhance paclitaxel-induced apoptosis.

Cationic liposomes are often used for their high transfection efficiency and biocompatibility [32]. We thus evaluated different cationic liposomes as delivery system for SBT-PEDF system. However, tested lipoplexes induced a decrease in ovarian cancer cell viability, especially when liposomes contain cholesterol. The incorporation of cholesterol into liposomes is known to improve the stability of the liposomal membrane in biologic fluids [35] and consequently, increase their capacity as delivery system [36], but it was not yet described to increase cytotoxicity of liposomes.

Alternatively, lipid biodegradable polymeric nanoparticles as lipid-based nanoparticles were described to display low or no toxicity

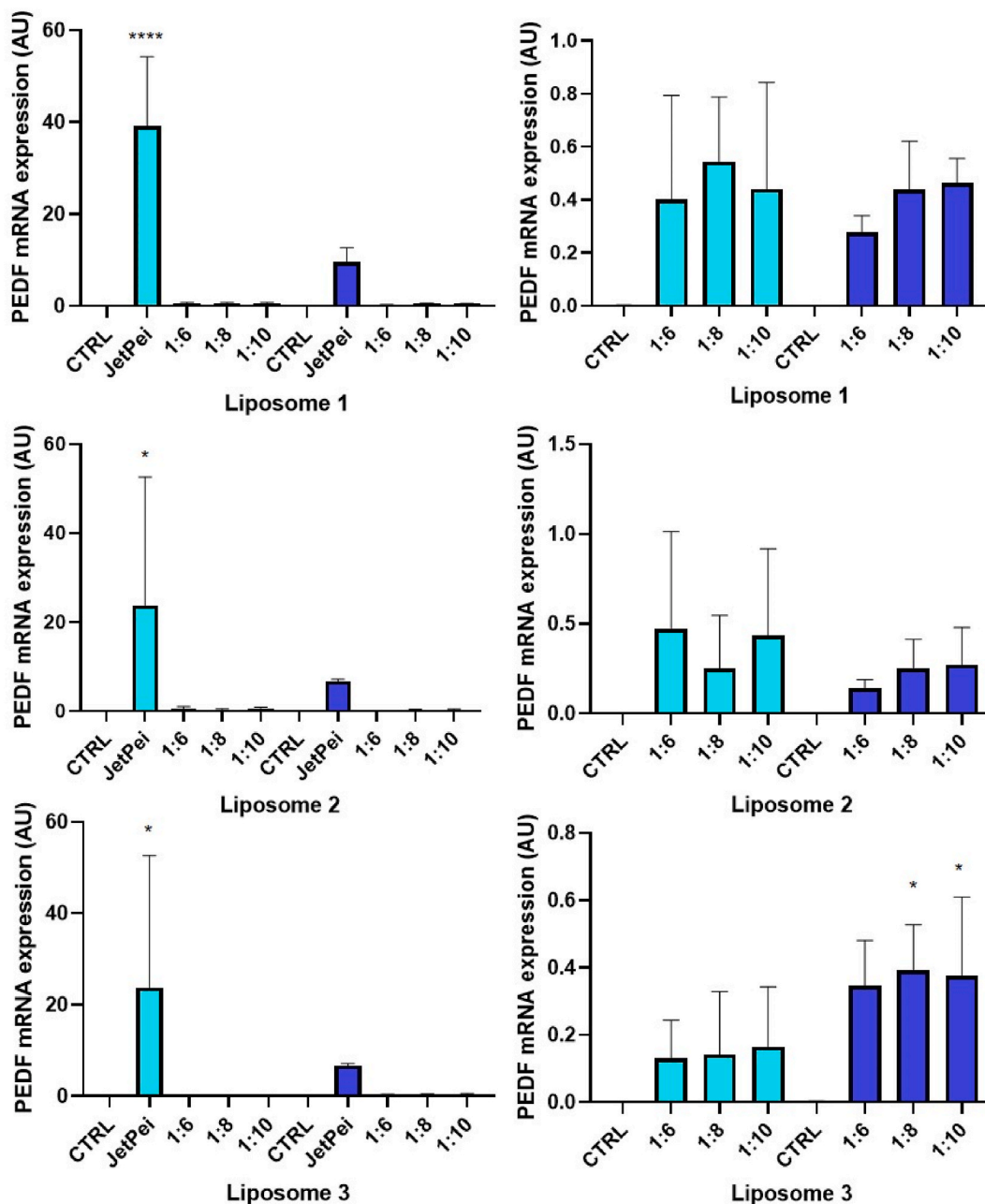


Fig. 3. Efficiency of liposomes. Transfection efficiency was determined by measuring PEDF gene expression by qPCR in transfected SKOV3 (light blue bars) and COV318 (dark blue bars) cells. Liposomes efficacy was compared to the commercial reagent JetPei. *p < 0.05; ****p < 0.0001 compared to the control.

[37,38]. We showed that their particle size and transfection efficiency in ovarian cancer cells were comparable to liposomes. As expected, the nanoliposome cytotoxicity is lower than liposome. In addition, the transfection efficiency of nanolipid is greater than that of liposome in ovarian cancer spheroids suggesting that nanolipid could be more efficient as gene delivery system than liposome in vivo. To confirm this hypothesis, we developed an ex vivo model of ovarian tumor culture as animal ethical replacement. We first used CAM to develop ovarian cancer tumors. CAM is an extraembryonic and highly vascularized membrane easily accessible. Within 3 days after ovarian cancer cell inoculation on CAM, ovarian tumor was formed. As the tumors were then excised at embryonic development day 14, the proposed model is classified as non-protected under the Animals Scientific Procedures, and is thus considered as a valid animal replacement technique. Tumors were then cultured in a mini bioreactor and transfected several times with SBT-PEDF using nanolipid 1 as delivery system. We determined that the use of this bioreactor allowed to maintain the tumor structure and viability

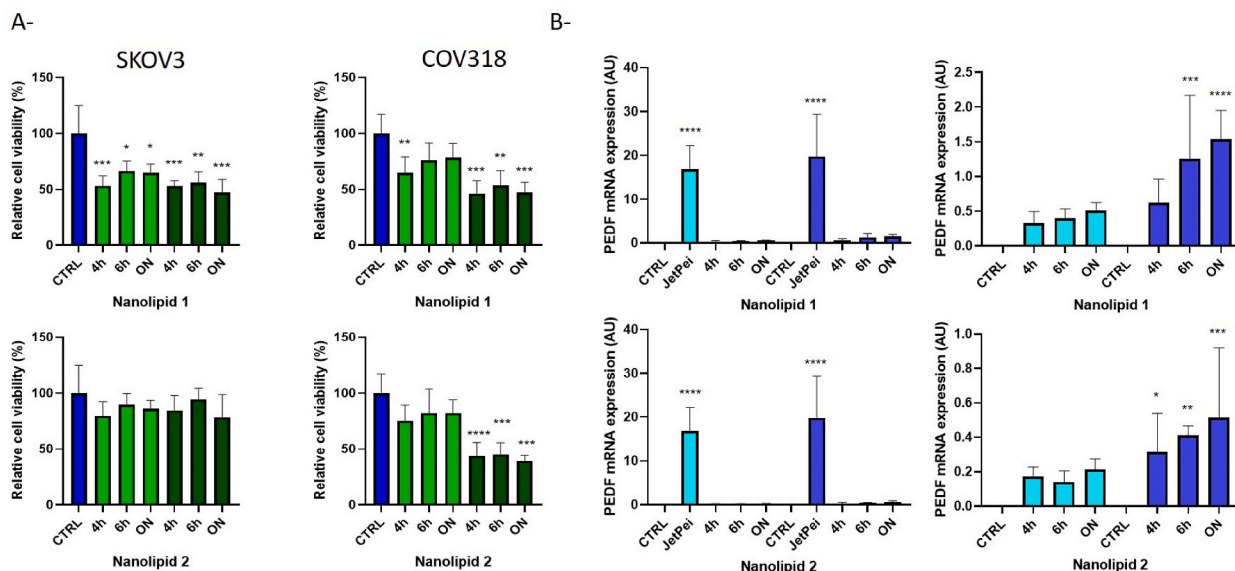


Fig. 4. Toxicity and efficiency of nanolipids. A- Effect of nanolipids (light green) and nanolipoplexes (dark green) on viability of SKOV3 and COV318 cells was evaluated by MTT assay. Results are expressed as mean ± SEM, n = 3. *p < 0.05; **p < 0.01; ***p < 0.001; ****p < 0.0001 compared to the control (CTRL, in blue). B- Transfection efficiency was determined by measuring PEDF gene expression by qPCR in transfected SKOV3 (light blue) and COV318 (dark blue) cells. Nanolipids efficacy was compared to the commercial reagent JetPei. ON: overnight

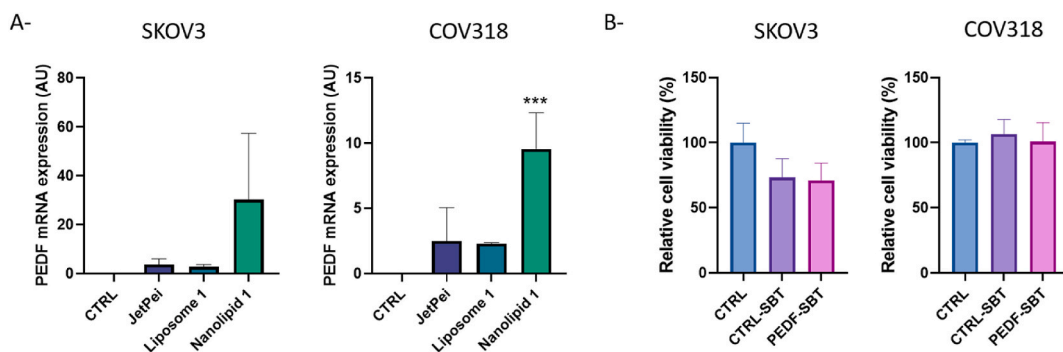


Fig. 5. Efficiency of liposome 1 and nanolipid 1 on ovarian cancer spheroids. A- Transfection efficiency was evaluated by measuring PEDF gene expression by qPCR in transfected SKOV3 (left panel) and COV318 (right panel) spheroids. B- Effect of nanolipoplexes on viability of SKOV3 (left panel) and COV318 (right panel) spheroids was evaluated by MTT assay. Results are expressed as mean ± SEM, n = 3. CTRL: Non transfected spheroids; CTRL-SBT: spheroids transfected with control SBT system; PEDF-SBT: spheroids transfected with PEDF transposon. ***p < 0.001 compared to the control.

until 8 days of culture. In addition, it allowed to consider the effects of shear stress on transfection efficiency.

Using this ex vivo model, we confirmed the efficiency of nanolipid to transfect PEDF-SBT system in tumors. Despite this model is not suitable to investigate the anti-angiogenic property of PEDF, we confirmed the anticancer potential of PEDF by demonstrating its synergistic effect on paclitaxel-induced apoptosis in tumors. Taken together, our findings suggest that the SBT-PEDF delivery nanolipid may be a promising candidate for intraperitoneal treatment of ovarian cancer.

5. Limitations of the study

The ex vivo transfection of tumors is interesting to evaluate the transfection efficiency of delivery systems or the effect of molecules on tumor’s cytotoxicity. However, this system is not suitable to evaluate effects of treatment on tumor angiogenesis or immune modulation. In addition, the stability of nanolipoplexes could be different in peritoneal fluid and in tumor’s culture medium.

Author contribution statement

Marie Cohen: Conceived and designed the experiments; Performed the experiments; Analyzed and interpreted the data;

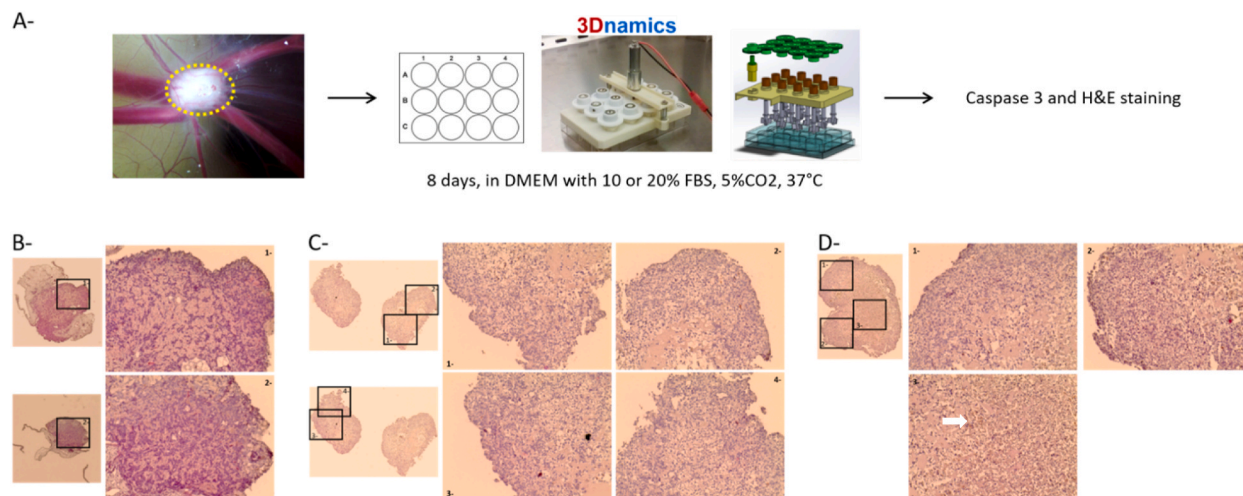


Fig. 6. Development of an ex vivo tumor assay. A- Experimental procedure for the culture of ovarian tumor for 8 days and evaluation of its impact on cell viability. SKOV3 cells were inoculated on CAM (2×10^6 cells per egg) and left for 6 days to form tumors. Tumors (outlined in yellow dotted line) were then extracted and cultured in 12-well plates covered by a miniaturized spinning bioreactor. Medium supplemented with 10% or 20% FBS was changed every 2 days and after 8 days in culture, tumors were collected, washed in PBS, fixed in formol and paraffin-embedded for histological analysis. B-D- Cleaved caspase 3 and H&E staining of tumors collected on CAM (B), after 8 days in culture with 10% FBS (C) or 20% FBS (D). The black boxed areas are shown at a higher magnification on the right. Original magnification X4 and $\times 20$ for the highest magnification. Arrow show cluster of cleaved caspase 3 positive cells. Image of spin Ω bioreactor was obtained from 3Dnamics, with authorization of use.

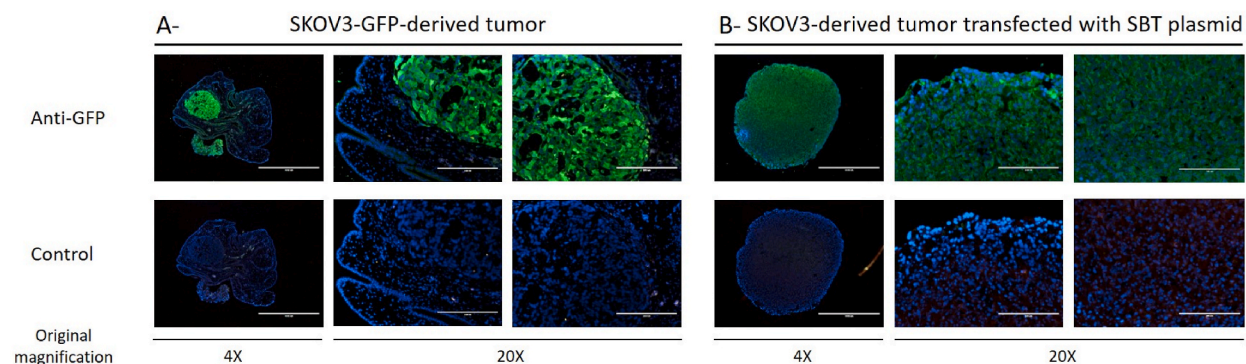


Fig. 7. Efficiency of nanopiplexes 1 on plasmids transfection in ovarian tumors. SKOV3-GFP-derived tumor (A) or SKOV3-derived tumor transfected with SBT plasmid (B) were labeled with anti-GFP (upper panel) or control (lower panel) antibodies and observed by fluorescence microscopy at different magnification. Scale bar represents 1000 μm for the lowest magnification and 200 μm for the highest magnification.

Contributed reagents, materials, analysis tools or data; Wrote the paper.

Pascale Ribaux: Performed the experiments; Analyzed and interpreted the data; Contributed reagents, materials, analysis tools or data.

Christine Wullemin: Performed the experiments.

Patrick Petignat; Florence Delie: Contributed reagents, materials, analysis tools or data.

Data availability statement

Data will be made available on request.

Declaration of interest's statement

The authors declare no conflict of interest.

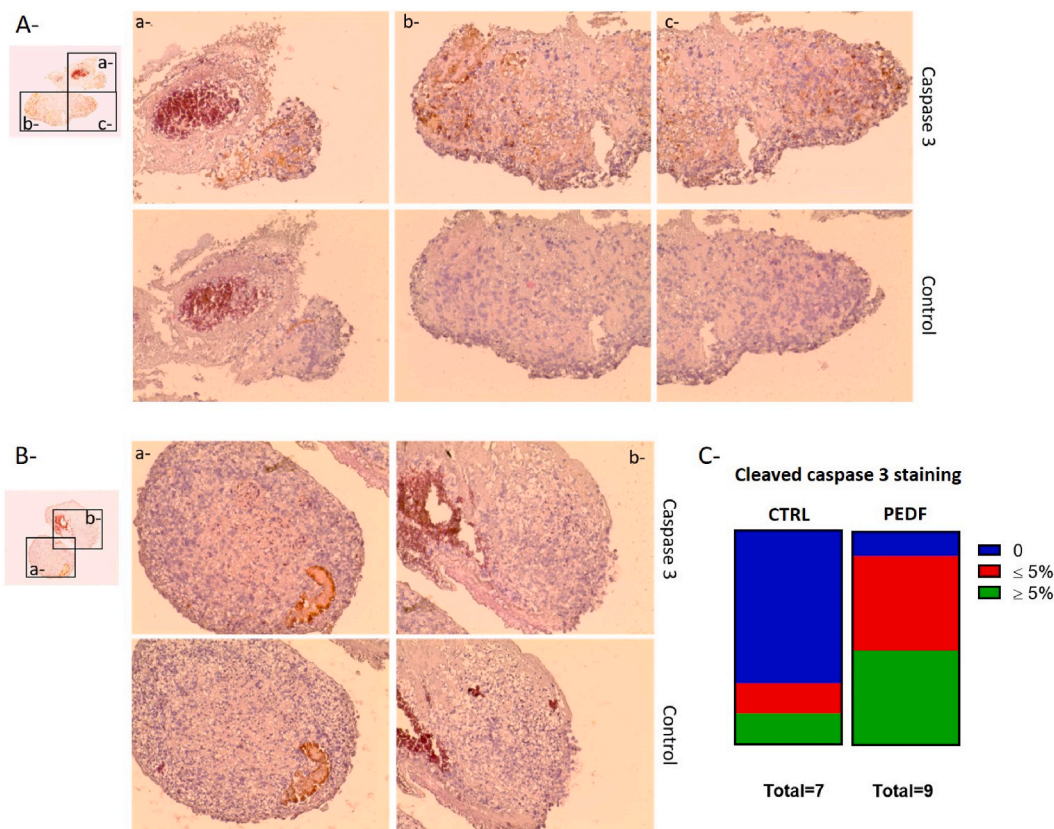


Fig. 8. Effect of PEDF on paclitaxel-treated ovarian tumors. Cleaved caspase 3 and H&E staining was performed on tumors transfected with PEDF transposon (A) or ctrl transposon (B) using nanolipid 1 as transfection reagent. The black boxed areas are shown at a higher magnification to the right. Original magnification $\times 4$ and $\times 20$ for the highest magnification. The graph (C) indicates the results of ctrl (n = 7) or PEDF transposon (n = 9) transfected tumors' staining depending on percentage of positive cells for cleaved caspase 3 staining.

Acknowledgments

This study was financially supported by funding from La Ligue Genevoise contre le Cancer, Helmut Horten foundation, Simone and Gustave Prevot foundation, and la foundation pour la lutte contre le cancer.

References

- [1] S.P. Becerra, V. Notario, The effects of PEDF on cancer biology: mechanisms of action and therapeutic potential, *Nat. Rev. Cancer* 13 (2013) 258–271, <https://doi.org/10.1038/nrc3484>.
- [2] Chuderland, Role of pigment epithelium-derived factor in the reproductive system - PubMed, (n.d.), <https://pubmed.ncbi.nlm.nih.gov/25049425/>. (Accessed 28 October 2022). accessed.
- [3] L. Belkacemi, S.X. Zhang, Anti-tumor effects of pigment epithelium-derived factor (PEDF): implication for cancer therapy. A mini-review, *J. Exp. Clin. Cancer Res.* 35 (2016) 4, <https://doi.org/10.1186/s13046-015-0278-7>.
- [4] Hjelmeland, *Mol Vis*, 1999, p. 33 (n.d.), <http://www.molvis.org/molvis/v5/a33/>. (Accessed 28 October 2022). accessed.
- [5] L.W.T. Cheung, S.C.L. Au, A.N.Y. Cheung, H.Y.S. Ngan, J. Tombran-Tink, N. Auersperg, A.S.T. Wong, Pigment epithelium-derived factor is estrogen sensitive and inhibits the growth of human ovarian cancer and ovarian surface epithelial cells, *Endocrinology* 147 (2006) 4179–4191, <https://doi.org/10.1210/en.2006-0168>.
- [6] N.J. Phillips, M.R. Ziegler, D.M. Radford, K.L. Fair, T. Steinbrueck, F.P. Xynos, H. Donis-Keller, Allelic deletion on chromosome 17p13.3 in early ovarian cancer, *Cancer Res.* 56 (1996) 606–611.
- [7] P. Ribaux, A. Britan, G. Thumann, F. Delie, P. Petignat, M. Cohen, Malignant ascites: a source of therapeutic protein against ovarian cancer? *Oncotarget* 10 (2019) 5894–5905, <https://doi.org/10.18632/oncotarget.27185>.
- [8] R. Ma, X. Chu, Y. Jiang, Q. Xu, Pigment Epithelium-Derived Factor, an Anti-VEGF Factor, Delays Ovarian Cancer Progression by Alleviating Polarization of Tumor-Associated Macrophages, *Cancer Gene Ther.*, 2022, <https://doi.org/10.1038/s41417-022-00447-4>.
- [9] D. Martinez-Marin, C. Jarvis, T. Nelius, W. de Riese, O.V. Volpert, S. Filleur, PEDF increases the tumoricidal activity of macrophages towards prostate cancer cells in vitro, *PLoS One* 12 (2017), e0174968, <https://doi.org/10.1371/journal.pone.0174968>.
- [10] M. Moradi-Chaleshtori, A. Koochaki, S. Shojaei, M. Paryan, M. Safarzadeh, S.M. Hashemi, S. Mohammadi-Yeganeh, Overexpression of pigment epithelium-derived factor in breast cancer cell-derived exosomes induces M1 polarization in macrophages, *Immunol. Lett.* 248 (2022) 31–36, <https://doi.org/10.1016/j.imlet.2022.05.005>.
- [11] M. Najafi, N. Hashemi Goradel, B. Farhood, E. Salehi, M.S. Nashtaei, N. Khanlarkhani, Z. Khezri, J. Majidpoor, M. Abouzaripour, M. Habibi, I.R. Kashani, K. Mortezaee, Macrophage polarity in cancer: a review, *J. Cell. Biochem.* 120 (2019) 2756–2765, <https://doi.org/10.1002/jcb.27646>.

- [12] Q. Gong, S. Qiu, S. Li, Y. Ma, M. Chen, Y. Yao, D. Che, J. Feng, W. Cai, J. Ma, X. Yang, G. Gao, Z. Yang, Proapoptotic PEDF functional peptides inhibit prostate tumor growth—a mechanistic study, *Biochem. Pharmacol.* 92 (2014) 425–437, <https://doi.org/10.1016/j.bcp.2014.09.012>.
- [13] L.P. Abramson, V. Stellmach, J.A. Doll, M. Cornwell, R.M. Arensman, S.E. Crawford, Wilms' tumor growth is suppressed by antiangiogenic pigment epithelium-derived factor in a xenograft model, *J. Pediatr. Surg.* 38 (2003) 336–342, <https://doi.org/10.1053/jpsu.2003.50104>; discussion 336–342.
- [14] A. Konson, S. Pradeep, R. Seger, Phosphomimetic mutants of pigment epithelium-derived factor with enhanced antiangiogenic activity as potent anticancer agents, *Cancer Res.* 70 (2010) 6247–6257, <https://doi.org/10.1158/0008-5472.CAN-10-0434>.
- [15] P. Subramanian, M. Deshpande, S. Locatelli-Hoops, S. Moghaddam-Taaheri, D. Gutierrez, D.P. Fitzgerald, S. Guerrier, M. Rapp, V. Notario, S.P. Becerra, Identification of pigment epithelium-derived factor protein forms with distinct activities on tumor cell lines, *J. Biomed. Biotechnol.* 2012 (2012), 425907, <https://doi.org/10.1155/2012/425907>.
- [16] S. Filleur, K. Volz, T. Nelius, Y. Mirochnik, H. Huang, T.A. Zaichuk, M.S. Aymerich, S.P. Becerra, R. Yap, D. Veliceasa, E.H. Shroff, O.V. Volpert, Two functional epitopes of pigment epithelium-derived factor block angiogenesis and induce differentiation in prostate cancer, *Cancer Res.* 65 (2005) 5144–5152, <https://doi.org/10.1158/0008-5472.CAN-04-3744>.
- [17] Y. Mirochnik, A. Aurora, F.T. Schulze-Hoepfner, A. Deabas, V. Shifrin, R. Beckmann, C. Polsky, O.V. Volpert, Short pigment epithelial-derived factor-derived peptide inhibits angiogenesis and tumor growth, *Clin. Cancer Res.* 15 (2009) 1655–1663, <https://doi.org/10.1158/1078-0432.CCR-08-2113>.
- [18] S.E. Crawford, P. Fitchew, D. Veliceasa, O.V. Volpert, The many facets of PEDF in drug discovery and disease: a diamond in the rough or split personality disorder? *Expert Opin. Drug Discov.* 8 (2013) 769–792, <https://doi.org/10.1517/17460441.2013.794781>.
- [19] Q. Chen, P. Cheng, N. Song, T. Yin, H. He, L. Yang, X. Chen, Y. Wei, Antitumor activity of placenta-derived mesenchymal stem cells producing pigment epithelium-derived factor in a mouse melanoma model, *Oncol. Lett.* 4 (2012) 413–418, <https://doi.org/10.3892/ol.2012.772>.
- [20] Y. Gao, A. Yao, W. Zhang, S. Lu, Y. Yu, L. Deng, A. Yin, Y. Xia, B. Sun, X. Wang, Human mesenchymal stem cells overexpressing pigment epithelium-derived factor inhibit hepatocellular carcinoma in nude mice, *Oncogene* 29 (2010) 2784–2794, <https://doi.org/10.1038/onc.2010.38>.
- [21] L. Yang, Y. Zhang, L. Cheng, D. Yue, J. Ma, D. Zhao, X. Hou, R. Xiang, P. Cheng, Mesenchymal stem cells engineered to secrete pigment epithelium-derived factor inhibit tumor metastasis and the formation of malignant ascites in a murine colorectal peritoneal carcinomatosis model, *Hum. Gene Ther.* 27 (2016) 267–277, <https://doi.org/10.1089/hum.2015.135>.
- [22] F.-Y. Cui, X.-R. Song, Z.-Y. Li, S.-Z. Li, B. Mu, Y.-Q. Mao, Y.-Q. Wei, L. Yang, The pigment epithelial-derived factor gene loaded in PLGA nanoparticles for therapy of colon carcinoma, *Oncol. Rep.* 24 (2010) 661–668.
- [23] L. Li, J. Yang, W.-W. Wang, Y.-C. Yao, S.-H. Fang, Z.-Y. Dai, H.-H. Hong, X. Yang, X.-T. Shuai, G.-Q. Gao, Pigment epithelium-derived factor gene loaded in rGD-PEG-PEI suppresses colorectal cancer growth by targeting endothelial cells, *Int. J. Pharm.* 438 (2012) 1–10, <https://doi.org/10.1016/j.ijpharm.2012.08.043>.
- [24] S.-S. He, Q.-J. Wu, C.Y. Gong, S.-T. Luo, S. Zhang, M. Li, L. Lu, Y.-Q. Wei, L. Yang, Enhanced efficacy of combination therapy with adeno-associated virus-delivered pigment epithelium-derived factor and cisplatin in a mouse model of Lewis lung carcinoma, *Mol. Med. Rep.* 9 (2014) 2069–2076, <https://doi.org/10.3892/mmr.2014.2117>.
- [25] H. Shi, L. Yang, W. Wei, X. Su, X. Li, M. Li, S. Luo, H. Zhang, L. Lu, Y. Mao, B. Kan, L. Yang, Systemically administered liposome-encapsulated Ad-PEDF potentiates the anti-cancer effects in mouse lung metastasis melanoma, *J. Transl. Med.* 11 (2013) 86, <https://doi.org/10.1186/1479-5876-11-86>.
- [26] T. Yu, B. Xu, L. He, S. Xia, Y. Chen, J. Zeng, Y. Liu, S. Li, X. Tan, K. Ren, S. Yao, X. Song, Pigment epithelial-derived factor gene loaded novel COOH-PEG-PLGA-COOH nanoparticles promoted tumor suppression by systemic administration, *Int. J. Nanomed.* 11 (2016) 743–759, <https://doi.org/10.2147/IJN.S97223>.
- [27] B. Xu, Q. Jin, J. Zeng, T. Yu, Y. Chen, S. Li, D. Gong, L. He, X. Tan, L. Yang, G. He, J. Wu, X. Song, Combined tumor- and Neovascular-"Dual targeting" gene/chemo-therapy suppresses tumor growth and angiogenesis, *ACS Appl. Mater. Interfaces* 8 (2016) 25753–25769, <https://doi.org/10.1021/acsami.6b08603>.
- [28] X. Bao, J. Zeng, H. Huang, C. Ma, L. Wang, F. Wang, X. Liao, X. Song, Cancer-targeted PEDF-DNA therapy for metastatic colorectal cancer, *Int. J. Pharm.* 576 (2020), 118999, <https://doi.org/10.1016/j.ijpharm.2019.118999>.
- [29] Y. Yang, L. He, Y. Liu, S. Xia, A. Fang, Y. Xie, L. Gan, Z. He, X. Tan, C. Jiang, A. Tong, X. Song, Promising nanocarriers for PEDF gene targeting delivery to cervical cancer cells mediated by the over-expressing FR α , *Sci. Rep.* 6 (2016), 32427, <https://doi.org/10.1038/srep32427>.
- [30] R.J.C. Bose, Y. Arai, J.C. Ahn, H. Park, S.-H. Lee, Influence of cationic lipid concentration on properties of lipid-polymer hybrid nanospheres for gene delivery, *Int. J. Nanomed.* 10 (2015) 5367–5382, <https://doi.org/10.2147/IJN.S87120>.
- [31] M.C. Bonnet, Immunohistological tools to discriminate apoptotic and necrotic cell death in the skin, in: K. McCall, C. Klein (Eds.), *Necrosis: Methods and Protocols*, Humana Press, Totowa, NJ, 2013, pp. 135–142, https://doi.org/10.1007/978-1-62703-383-1_10.
- [32] C. Liu, L. Zhang, W. Zhu, R. Guo, H. Sun, X. Chen, N. Deng, Barriers and strategies of cationic liposomes for cancer gene therapy, *Mol. Ther. Meth. Clin. Develop.* 18 (2020) 751–764, <https://doi.org/10.1016/j.omtm.2020.07.015>.
- [33] N.T. Jarzubska, S. Lauchli, C. Iselin, L.E. French, P. Johansen, E. Guenova, T.M. Kündig, S. Pascolo, Functional differences between protamine preparations for the transfection of mRNA, *Drug Deliv.* 27 (2020) 1231–1235, <https://doi.org/10.1080/10717544.2020.1790692>.
- [34] B.P. Rickard, C. Conrad, A.J. Sorrin, M.K. Ruhi, J.C. Reader, S.A. Huang, W. Franco, G. Scarcelli, W.J. Polachek, D.M. Roque, M.G. del Carmen, H.-C. Huang, U. Demirci, I. Rizvi, Malignant ascites in ovarian cancer: cellular, acellular, and biophysical determinants of molecular characteristics and therapy response, *Cancers* 13 (2021) 4318, <https://doi.org/10.3390/cancers13174318>.
- [35] S. Vemuri, C.T. Rhodes, Preparation and characterization of liposomes as therapeutic delivery systems: a review, *Pharm. Acta Helv.* 70 (1995) 95–111, [https://doi.org/10.1016/0031-6865\(95\)00010-7](https://doi.org/10.1016/0031-6865(95)00010-7).
- [36] C. Kirby, G. Gregoriadis, The effect of the cholesterol content of small unilamellar liposomes on the fate of their lipid components in vivo, *Life Sci.* 27 (1980) 2223–2230, [https://doi.org/10.1016/0024-3205\(80\)90388-4](https://doi.org/10.1016/0024-3205(80)90388-4).
- [37] B. García-Pinel, C. Porras-Alcalá, A. Ortega-Rodríguez, F. Sarabia, J. Prados, C. Melguizo, J.M. López-Romero, Lipid-based nanoparticles: application and recent advances in cancer treatment, *Nanomaterials* 9 (2019) 638, <https://doi.org/10.3390/nano9040638>.
- [38] S. Scioli Montoto, G. Muraca, M.E. Ruiz, Solid lipid nanoparticles for drug delivery: pharmacological and biopharmaceutical aspects, *Front. Mol. Biosci.* 7 (2020). <https://www.frontiersin.org/articles/10.3389/fmolb.2020.587997>. (Accessed 1 November 2022). accessed.